Anisotropic enhanced backscattering induced by anisotropic diffusion

B. P. J. Bret* and A. Lagendijk
Universiteit Twente, Postbus 217, 7500AE Enschede, The Netherlands
(Received 2 April 2004; published 3 September 2004)

The enhanced backscattering cone displaying a strong anisotropy from a material with anisotropic diffusion is reported. The constructive interference of the wave is preserved in the helicity preserving polarization channel and completely lost in the nonpreserving one. The internal reflectivity at the interface modifies the width of the backscatter cone. The reflectivity coefficient is measured by angular-resolved transmission. This interface property is found to be isotropic, simplifying the backscatter cone analysis. The material used is a macroporous semiconductor, gallium phosphide, in which pores are etched in a disordered position but with a preferential direction.

DOI: 10.1103/PhysRevE.70.036601 PACS number(s): 42.25.Dd

I. INTRODUCTION

Study of light propagation through strongly scattering media strongly intensified after the discovery that interference plays a role even after numerous scattering events. Light, as well as electrons, sound, etc., displays through its wave nature an entire new realm of effects which are not present in the diffusion regime. Among those interesting and dramatic phenomena, we find speckle statistics, studied in theory [1], and experimentally, for microwaves [2] and for optical wavelengths [3]. Another interference phenomenon, enhanced backscattering (EBS), has been thoroughly studied both theoretically [4–6] and experimentally [7–10]. When interference dominates, Anderson localization [11], the breakdown of transport due to interference, sets in, as has been reported in Refs. [9,12,13].

Porous gallium phosphide (GaP) has already been known for a few years as the strongest scattering material for visible light [14] and has recently been proved to be displaying a very strong anisotropy in diffusion [15]. Anisotropic diffusion means that light propagates further and faster in one direction ($\parallel$) than in the two others ($\perp$).

In this paper, we present two types of measurements on anisotropic materials: angular resolved transmission (ART) and EBS. Samples are prepared in a similar way as in Ref. [15] and some of the previous results have been reproduced for consistency.

From the ART measurement it is in principle possible to determine the reflectivity properties of the interface of the material. Unfortunately, no quantitative agreement between these measurements on anisotropic material and state-of-the-art theory was found (see Refs. [16,17] for the theory and especially Ref. [18] for the good agreement between theory and isotropic porous GaP). Nevertheless, the ART measurements can be used for further interpretation of EBS measurements. EBS results in the increase, up to a factor 2, of the intensity in the exact backscatter direction arising from constructive interference of time-reversed paths. It is characteristic of any wave being multiply scattered. The theory of EBS, with extensions to take internal reflectivity into account, can be found in Refs. [6,19]. The full width at half maximum (FWHM) of the EBS cone is found to be

$$\theta_{\mathrm{FWHM}} \approx \frac{0.7}{k_0 \ell}(1-R), \tag{1}$$

where k_0 is the wave number of light in vacuum, ℓ is the transport mean free path of the material, and R an (average) reflectivity coefficient of the interface, which can be calculated from diffusion theory and Fresnel coefficients [17].

We find an anisotropic backscatter cone, that is to say a different line shape of backscattered light for scans parallel and perpendicular to the axis of the sample. This anisotropy in the backscatter cone is due to multiple scattering of light. Indeed, isotropic multiple scattering leads to an isotropic backscatter cone and anisotropic diffusion leads to an anisotropic backscatter cone. Other effects, which are here considered trivial due to first orders in scattering, are the polarization anisotropy [20] and the backscattering effect in the nonpreserving polarization channels [7,8,21]. These other effects are discussed briefly in following sections.

II. SAMPLES

The anisotropic material [15] is synthesized by anodic etching of a wafer of GaP. A cleaved edge, instead of the surface of the wafer, is put in contact with the electrolyte (see Fig. 1). This geometry implies that the pores grow along the wafer, parallel to the surface, and not normal to it. The plane of the surface contains both directions, parallel and normal to the etching axis. We therefore expect anisotropy in measurements performed in a plane either parallel or orthogonal to the etching axis. The thickness of the wafer is 310 μm. The etching process goes on sufficiently long so that possible edge effects are negligible. The samples are then 2 mm long, much bigger than all other typical length scales. The samples are therefore in a slab geometry. The distribution of pores in the whole bulk of the sample is found to be homogeneous [15].

The samples are made by applying a 10.5-V potential on one (cleaved) edge of the wafer, and letting the opposite edge

*Electronic address: b.p.j.bret@utwente.nl

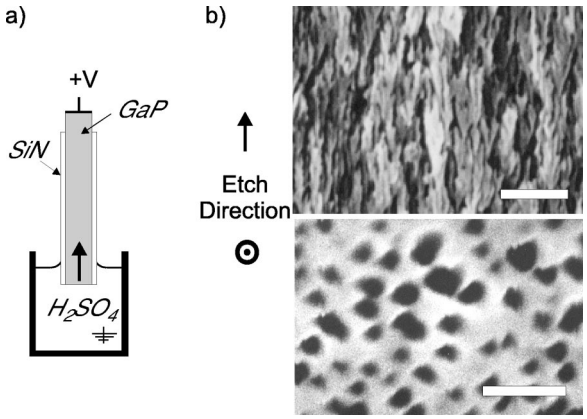

FIG. 1. (a) Cartoon of the etching setup. Pores are grown from the bottom up, parallel to the surface of the wafer. (b) Two cross sections, as SEM images, showing the elongation of the pore structure. The top image is parallel and the bottom image is normal to the etching direction. Scale bars =1 μm.

be in contact with a 0.5-mol/L sulfuric acid, electrically grounded, solution. The remaining four sides are covered by a 200-nm-thick layer of silicon nitride (SiN), to prevent unwanted side etching. The obtained samples display a porosity of 46% and the diameter of the pores is 70 ± 30 nm. A scanning electron microscopy (SEM) image of a typical sample is shown in Fig. 1. The random nature of the pores, their small diameter, and the high refractive index contrast (3.3 for GaP at 633 nm against air) ensures that light will be strongly scattered. Furthermore, the elongation of the pores, being several times their diameter, induces the anisotropy for light scattering and diffusion.

III. DIFFUSION MEASUREMENTS

The most straightforward measurement to show anisotropic diffusion in a slab is letting a pointlike light source on one side of the slab diffuse to the other side, spreading unevenly in different directions. The principle of such measurements is described in Refs. [15,22,23]. A helium-neon laser beam (633 nm) is focused on one side of the sample, with a focus of 10 μm, and the other side of the sample is imaged on a charge-coupled device (CCD) camera (see Fig. 2). Light propagating through the sample gets diffuse after one transport mean free path, losing memory of its initial polarization along with its initial direction. In transmission through thick turbid material, the incident polarization will therefore play no role. Two cross sections of the image are taken, going through the center of the spot and in the $\parallel$ and $\perp$ directions, respectively, and fit to a Gaussian [15]. The ratio of spot widths is found to be $W_{\parallel}/W_{\perp}=2.1\pm0.2$, in agreement with Ref. [15].

Angular-resolved transmission measurements [18] on anisotropic samples have been performed. The sample is illuminated at normal incidence by a helium-neon laser beam. The incident polarization has again no effect on the transmission. The internal reflection of one particular interface is an intrinsic parameter which does not depend on which side of the sample light impinges on. This parameter is equal for

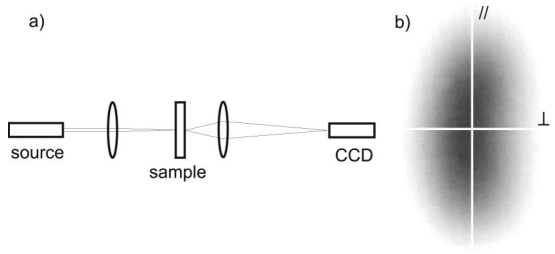

FIG. 2. (a) Transmitted spot imaging setup cartoon. (b) Image recorded on the CCD camera, for an anisotropic sample, with inverted gray scale: darker region corresponds to higher light intensity recorded. Two white lines indicates the useful cross sections. The anisotropy of the spot directly corresponds to anisotropy diffusion.

front and back interfaces in our samples since they are symmetrical. The intensity of light escaping the sample from the other side is measured as a function of angle. Both polarization directions P (electrical field vector parallel to detection plane) and S (vector normal to plane) are recorded. The sample can be oriented with the direction of the pores in the plane of detection ($\parallel$), or normal to it ($\perp$). Several measurements for each orientation and polarization are performed, changing the position of the sample each time in order to average over disorder. Figure 3 shows the results, for two orientations and two polarizations. No difference in angular dependence between the two sets, $\parallel$ and $\perp$, can be found within the experimental uncertainty. We estimate the uncertainty as 5%. This insures that the interface properties, extrapolation length [16] and reflectivity coefficient R, are isotropic, in accordance with intuition. EBS measurements, as seen from Eq. (1), depend on R. R being isotropic, the comparison of the here obtained anisotropic EBS widths will lead to comparison of the mean free paths.

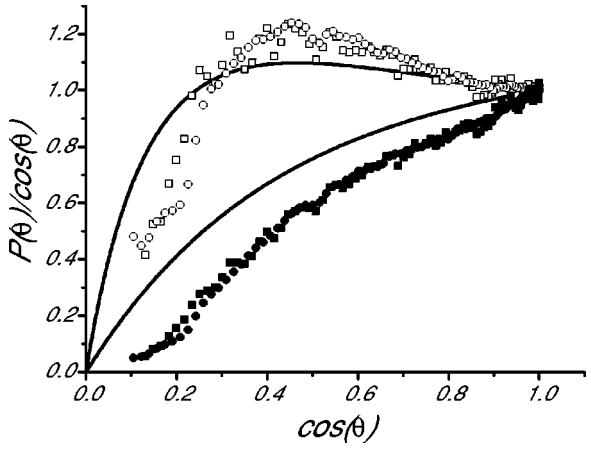

FIG. 3. Transmitted intensity, $P(\theta)$ over $\cos(\theta)$ as a function of angle θ of an anisotropic sample in two orientations, etching direction in (circles) and out (squares) of scanning plane and for two polarizations, P (open symbols) and S (closed symbols). The two full curves are closest fit to the theory, with $n=2.45$. The experimental data are independent of direction: the reflectivity properties are isotropic in this sample, but they do not fit with the isotropic theory.

ART measurements can be compared to the theory found in Refs. [16,17] which predicts the shape of the ART depending on the effective refractive index of the material. Both polarizations of the best fit to this theory, with a refractive index of 2.45, are plotted by full lines in Fig. 3. Unfortunately, no satisfying quantitative agreement can be found between our measurements and the theory within experimental accuracy. We interpret this discrepancy as being due to the presence of two extra layers on top of the porous structure. Indeed, the pores cannot touch the surface of the wafer, which leads to a typically 200-nm thin layer of bare GaP between the pores and the surface of the wafer. Such a layer has been found [18] to significantly change the ART. The second layer is the remaining SiN layer used to protect the surfaces against etching, and which cannot be removed without damage to the samples. This lack of fit of our measurements with the theory does not allow us to quote an exact value for the reflectivity coefficient of the interface of the samples.

IV. ENHANCED BACKSCATTERING IN HELICITY PRESERVING CHANNEL

EBS measurements have been performed using the off-centered rotation technique [24] and a helium-neon laser as light source. This setup allows us to horizontally scan the angle from the exact backscattered direction, with a 900-mrad range and an 0.5-mrad resolution with an illumination area 2 mm in diameter. The measured sample can be oriented with etching direction either vertical ($\perp$) or horizontal ($\parallel$), so that the etching direction is either normal or parallel to the scanning plane. In order to average over disorder, a nutation is applied on the sample. The range of the nutation is less than 150 mrad. Further averaging was done by making measurements at four different positions of the samples.

It is possible to measure EBS with various polarizations. Relevant are linear polarization, with parallel or orthogonal analyzer, and circular, with helicity preserving or nonpreserving. Using linear polarization, although experimentally easier to perform, is the least preferable solution for our goal. Indeed, in addition to parallel and cross analyzers, we can orient the incident linear polarization either parallel or orthogonal to the pores. Furthermore, it has already been noticed [20] that an incoming linear polarization in or normal to the scanning plane also introduced an anisotropy in the backscatter cone, due to a trivial polarization effect and not anisotropic diffusion. The authors [20] measured the EBS from concentrated suspensions of polystyrene spheres in the linear (and parallel) polarization channel. The direction of the incident polarization was shown to break the rotational symmetry of the setup and to imply a distinction between two different directions, parallel and orthogonal to the polarization. The measured backscatter cone displayed different widths along these two directions. The anisotropy in Ref. [20] is due to the vector nature of light.

In order to avoid this polarization anisotropy of the backscatter cone, the circular polarization channels can be used. In addition, the helicity preserving channel filters out the single-scattering contribution. This effectively reduces the background of the EBS cone, and ultimately allows us to reach the theoretical enhancement factor of 2 [25]. In the present study, the enhancement factor does not reach 2. This is due to paths for light which leave the sample outside the illuminated area but still fall on the detector. In the helicity nonpreserving channel, only the low orders of scattering remain and contribute to a (much) smaller enhancement factor.

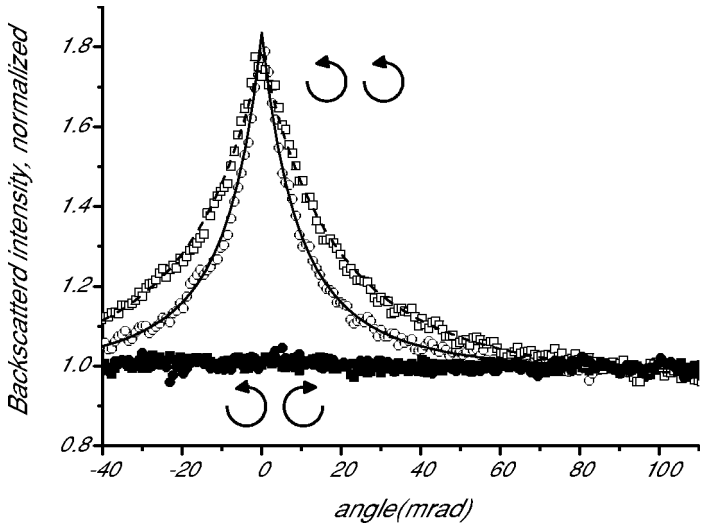

FIG. 4. Backscattered intensity as a function of angle, normalized to 1 at high angles, of an anisotropic sample in two orientations. Etching direction in (circles) and out (squares) of scanning plane, and two polarizations, helicity preserving (open symbols) and nonpreserving (closed symbols). The lines are fit to the isotropic theory [19,26]. The anisotropy is easily seen in the preserving channel, which implies anisotropic wave diffusion.

Figure 4 shows EBS measurements on an anisotropic sample, for the two possible orientations, and for the two circular polarization channels. In the helicity preserving channel (open symbols) the backscatter cone is clearly visible and strongly anisotropic. Using the line shape predicted in the isotropic case [19,26], each curve taken separately can be fit in order to give two different mean free paths. The two fits yield a good agreement, within experimental accuracy. Since circular polarization is used and since the reflectivity coefficient R is found to be isotropic, it can be concluded, following Eq. (1), that the ratio of the widths is the inverse of the ratio of the mean free paths. So from these fits, the ratio of transport mean free paths is found to be $\ell_{\parallel}/\ell_{\perp} = 1.90 \pm 0.15$.

Although we are not able to measure directly the reflectivity coefficient R, we can deduce a good estimate. Indeed, we find in Ref. [18] measurements on samples which are similar to our own except for the etching direction which is in that case normal to the surface. Those measurements showed that the bulk of such a material has an effective refractive index of 1.40 ± 0.05. An interface between a diffusive material with such refractive index and air would have an extrapolation ratio [16] $z_e = 1.97 \pm 0.22$ and a reflectivity coefficient $R = 0.49 \pm 0.04$. Our samples have two additional interfaces, coming from the extra GaP layer and the SiN coating, having respectively 3.3 and 2.0 as refractive index. Taking these into account, we find $z_e = 2.95 \pm 0.20$ and

$R=0.63\pm0.03$. Using these latter values to interpret our experiment, we find $\ell_{\parallel}=1.52\pm0.07$ μm and $\ell_{\perp}=0.80\pm0.04$ μm.

V. ENHANCED BACKSCATTERING IN HELICITY NONPRESERVING CHANNEL

Before discussing our measurements on EBS in the helicity nonpreserving channel, we will review shortly the experimental and theoretical literature on the subject.

The EBS cone has been shown to exist in the cross polarized (linear) channel in the case of Rayleigh scatterers and to disappear with increasing anisotropy of the scatterers [21]. It has also been shown to exist in the helicity nonpreserving channel in the case of Rayleigh scatterers and to disappear with optical activity [27].

Measurements on nematic liquid crystals [28,29] show the absence of cone, within 1%, in the cross polarized channel, or an enhancement factor evaluated to 3% [30]. A backscatter cone in the linear orthogonal channel has been measured [31] from both 0.2- and 1-μm-diameter polystyrene spheres suspensions, with enhancement of respectively 10% and 20%. EBS cones in the linear orthogonal and in the helicity nonpreserving channels of a cloud of cold Rubidium atoms were reported [32].

Nematic liquid crystals are very anisotropic scatterers and are birefringent. Both effects contribute to the reduction of the enhancement factor in the cross polarized channel. Spherical colloids are neither very anisotropic nor birefringent, and therefore display an enhancement in the cross polarized channel. The physics of the EBS cone in cold atoms is beyond the reach of the classical theories mentioned here [21,27].

Our measurements in the helicity nonpreserving channel, as seen from the filled symbols in Fig. 4, do not show any observable EBS cone, for both orientations of the sample. The enhancement factor is here smaller than 2%. The scattering in porous GaP is very anisotropic, reducing the expected enhancement factor. Considering optical activity, the enhancement would vanish for $\ell \gg \lambda/\Delta n$, where Δn is the difference in refractive index for the two circular polarizations, and λ the wavelength in vacuum. Applying this condition to our samples implies $\Delta n \gg 1/2$, which, compared to an effective refractive index around 1.5, seems unrealistically large.

VI. CONCLUSIONS

We have synthesized a very strongly scattering material which displays strong anisotropic diffusion. The anisotropy is shown by a stationary diffusion method, and the interface properties are found to remain isotropic. We measure a strongly anisotropic enhanced backscattering cone due to the anisotropy in the diffusion of waves. During preparation of this paper, the measurement of an anisotropic backscattering cone in nematic liquid crystals was presented by Sapienza *et al.* [29]. The experiment presented in their paper is very convincing.

In the present paper as well as in the work of Sapienza *et al.*, a theory which encompasses the anisotropy in diffusion, needed to really interpret an anisotropic EBS cone, is lacking. Ongoing work [33] suggests it cannot be derived from the isotropic case in an intuitive manner.

ACKNOWLEDGMENTS

We would like to thank Patrick Johnson and Karin Overgaag for experimental help and discussions. This work is part of the research program of the "Stichting voor Fundamenteel Onderzoek der Materie" (FOM), which is financially supported by the "Nederlands Organisatie voor Wetenschappelijk Onderzoek" (NWO).

[1] B. A. van Tiggelen, P. Sebbah, M. Stoytchev, and A. Z. Genack, Phys. Rev. E **59**, 7166 (1999).
[2] A. Z. Genack, P. Sebbah, M. Stoytchev, and B. A. van Tiggelen, Phys. Rev. Lett. **82**, 715 (1999).
[3] P. M. Johnson, A. Imhof, B. P. J. Bret, J. Gómez Rivas, and A. Lagendijk, Phys. Rev. E **68**, 016604 (2003).
[4] E. Akkermans, P. E. Wolf, R. Maynard, and G. Maret, J. Phys. (France) **49**, 77 (1988).
[5] E. Akkermans, P. E. Wolf, and R. Maynard, Phys. Rev. Lett. **56**, 1471 (1986).
[6] M. B. van der Mark, M. P. van Albada, and A. Lagendijk, Phys. Rev. B **37**, 3575 (1988).
[7] M. P. van Albada and A. Lagendijk, Phys. Rev. Lett. **55**, 2692 (1985).
[8] P. E. Wolf and G. Maret, Phys. Rev. Lett. **55**, 2696 (1985).
[9] F. J. P. Schuurmans, M. Megens, D. Vanmaekelbergh, and A. Lagendijk, Phys. Rev. Lett. **83**, 2183 (1999).
[10] J. Gómez Rivas, R. W. Tjerkstra, D. Vanmaekelbergh, J. J. Kelly, and A. Lagendijk, Appl. Phys. Lett. **80**, 4498 (2002).
[11] See, for instance, P. Sheng, *Introduction to Wave Scattering, Localization, and Mesoscopic Phenomena* (Academic, New York, 1995).
[12] D. S. Wiersma, P. Bartolini, A. Lagendijk, and R. Righini, Nature (London) **390**, 671 (1997).
[13] See also F. Scheffold, R. Lenke, R. Tweer, and G. Maret, Nature (London) **398**, 206 (1999); D. S. Wiersma, J. Gómez Rivas, P. Bartolini, A. Lagendijk, and R. Righini, *ibid.* **398**, 207 (1999).
[14] F. J. P. Schuurmans, D. Vanmaekelbergh, J. van de Lagemaat, and A. Lagendijk, Science **284**, 141 (1999).
[15] P. M. Johnson, B. P. J. Bret, J. Gómez Rivas, J. J. Kelly, and A. Lagendijk, Phys. Rev. Lett. **89**, 243901 (2002).
[16] J. X. Zhu, D. J. Pine, and D. A. Weitz, Phys. Rev. A **44**, 3948 (1991).
[17] M. U. Vera and D. J. Durian, Phys. Rev. E **53**, 3215 (1996).
[18] J. Gómez Rivas, D. H. Dau, A. Imhof, R. Sprik, B. P. J. Bret, P. M. Johnson, T. W. Hijmans, and A. Lagendijk, Opt. Commun. **220**, 17 (2003).

[19] A. Lagendijk, R. Vreeker, and P. de Vries, Phys. Lett. A **136**, 81 (1989).
[20] M. P. van Albada, M. B. van der Mark, and A. Lagendijk, Phys. Rev. Lett. **58**, 361 (1987).
[21] M. J. Stephen and G. Cwilich, Phys. Rev. B **34**, 7564 (1986).
[22] M. H. Kao, K. A. Jester, A. G. Yodh, and P. J. Collings, Phys. Rev. Lett. **77**, 2233 (1996).
[23] D. S. Wiersma, A. Muzzi, M. Colocci, and R. Righini, Phys. Rev. Lett. **83**, 4321 (1999).
[24] D. S. Wiersma, M. P. van Albada, and A. Lagendijk, Rev. Sci. Instrum. **66**, 5473 (1995).
[25] D. S. Wiersma, M. P. van Albada, B. A. van Tiggelen, and A. Lagendijk, Phys. Rev. Lett. **74**, 4193 (1995).
[26] P. den Outer, Ph.D. thesis, Universiteit van Amsterdam, 1995.
[27] F. C. MacKintosh and S. John, Phys. Rev. B **37**, 1884 (1988).
[28] H. K. M. Vithana, L. Asfaw, and D. L. Johnson, Phys. Rev. Lett. **70**, 3561 (1993).
[29] R. Sapienza, S. Mujumdar, C. Cheung, A. G. Yodh, and D. Wiersma, Phys. Rev. Lett. **92**, 033903 (2004).
[30] L. V. Kuzmin, V. P. Romanov, and L. A. Zubkov, Phys. Rev. E **54**, 6798 (1996).
[31] M. P. van Albada, M. B. van der Mark, and A. Lagendijk, J. Phys. D **21**, 28 (1988).
[32] G. Labeyrie, F. de Tomasi, J.-C. Bernard, C. A. Müller, C. Miniatura, and R. Kaiser, Phys. Rev. Lett. **83**, 5266 (1999).
[33] A. Lagendijk (private communication).